Anal Bioanal Chem (2016) 408:4329–4339
DOI 10.1007/s00216-016-9532-x

RESEARCH PAPER

Electrochemical biosensing of galactose based on carbon materials: graphene versus multi-walled carbon nanotubes

Berna Dalkıran[1] · **Pınar Esra Erden**[1] · **Esma Kılıç**[1]

Received: 11 January 2016 / Revised: 6 March 2016 / Accepted: 30 March 2016 / Published online: 13 April 2016

Abstract In this study, two enzyme electrodes based on graphene (GR), Co_3O_4 nanoparticles and chitosan (CS) or multi-walled carbon nanotubes (MWCNTs), Co_3O_4 nanoparticles, and CS, were fabricated as novel biosensing platforms for galactose determination, and their performances were compared. Galactose oxidase (GaOx) was immobilized onto the electrode surfaces by crosslinking with glutaraldehyde. Optimum working conditions of the biosensors were investigated and the analytical performance of the biosensors was compared with respect to detection limit, linearity, repeatability, and stability. The MWCNTs-based galactose biosensor provided about 1.6-fold higher sensitivity than its graphene counterpart. Moreover, the linear working range and detection limit of the MWCNTs-based galactose biosensor was superior to the graphene-modified biosensor. The successful application of the purposed biosensors for galactose biosensing in human serum samples was also investigated.

Keywords Amperometry · Co_3O_4 nanoparticles · Galactose biosensor · Graphene · Multi-walled carbon nanotubes

Introduction

Electrochemical biosensors based on nanomaterials including metal or metal oxide nanoparticles, carbon nanotubes, and graphene have recently been investigated intensively, due to the extraordinary chemical and physical properties of these materials [1–3]. CNTs are fascinating materials for sensing applications due to several properties like small dimensions, high surface area, mechanical strength, high electrical conductivity, good biocompatibility, functional surface, and good chemical stability [4]. Similarly to carbon nanotubes, graphene two-dimensional layer of graphite with sp^2 carbon atoms arranged in a hexagonal lattice has also demonstrated attractive application in electrochemical biosensing because of the unique properties including fast electron transfer kinetics, excellent thermal conductivity, high specific surface area, and good biocompatibility [5].

Many types of metal oxides, such as Fe_3O_4, Al_2O_3, Co_3O_4, and TiO_2, have been used to construct biosensors [3]. Among them, Co_3O_4 nanoparticles represent an excellent material with low cost, wide availability, and excellent electrocatalytic properties [6]. The use of metal oxide nanoparticles was reported to improve the response time, linear range, detection limit, reproducibility, and long-term stability of the biosensors [7].

The nanocomposites combining different components are expected to further improve the characteristics of each component, leading to promising applications in electrochemical biosensing. Up to now, various metal oxide–graphene or metal oxide–carbon nanotube nanocomposites such as TiO_2–graphene [8], Fe_3O_4–graphene [9], ZnO–graphene [10], Fe_3O_4–MWCNTs [11], silver nanoparticles–CNTs [12], and Co_3O_4–MWCNTs [13] have been reported as the base for biosensor construction.

The determination of galactose is important in food science, human nutrition, fermentation industry, and medicine [14]. Elevated levels of galactose in blood and urine can be a symptom of galactosemia, galactosuria, and other metabolic disorders [15, 16]. Galactosemia is a genetically inherited metabolic disorder characterized by an inability of the body to

✉ Esma Kılıç
ekilic@science.ankara.edu.tr

[1] Faculty of Science, Department of Chemistry, Ankara University, 06100 Tandoğan, Ankara, Turkey

utilize galactose [17]. People with galactosemia have very little or entirely lack enzymes that help to metabolize galactose. Restriction of dietary galactose is the mainstay of treatment. Milk and dairy products are the most common food source of galactose, thus people with galactosemia should avoid these foods [18]. When the blood level is more than 1.1 mM in neonatal infant, it becomes fatal galactosemia [19]. If galactosemia is not treated, infants with this condition may develop cataracts, liver diseases and kidney problems, brain damage, and in some cases, even death [20]. Therefore, development of simple, accurate, low cost, rapid, and practical methods is necessary to analyze galactose in clinical laboratories.

Among the various methods available for determination of galactose such as chromatography, fluorimetry, and spectrophotometry [21–24], electrochemical biosensors are rapid, economic, highly sensitive, and specific [25–27].

Galactose oxidase, a member of radical-coupled copper oxidases family with broad substrate specificity, catalyzes the conversion of galactose to hydrogen peroxide and galactonic acid [28–30]. Enzymatically produced H_2O_2 can be detected electrochemically by amperometric electrodes, either by measuring the anodic or cathodic response, due to the oxidation or reduction of H_2O_2 at the surface of the working electrode, respectively. Different amperometric biosensors have been reported for the detection of galactose [16, 17, 19, 26, 27, 31].

A survey in the literature indicates that there are only a few studies where the performance of CNTs and graphene-based electrodes are compared for various biosensors [32–34], and to the best of our knowledge, there is no comparison of graphene and MWCNTs-based electrodes for the electrochemical biosensing of galactose. In this work, we fabricated two effective galactose biosensors based on MWCNTs/Co_3O_4/CS and GR/Co_3O_4/CS nanocomposite-modified glassy carbon electrodes. The analytical performance of the biosensors was compared with respect to detection limit, linearity, and interference caused by potential interfering substances. The successful application of the purposed biosensors for galactose biosensing in real samples was also described.

Materials and methods

Reagents

Galactose oxidase (from Dactylium dendroides), Co_3O_4 nanoparticles (<50 nm particle size), potassium hexacyanoferrate (III), potassium hexacyanoferrate (II), uric acid, galactose, dopamine, chitosan, methionine, urea, creatinine, ascorbic acid, aspartic acid, nafion, and glutaraldehyde were purchased from Sigma-Aldrich (St. Louis, MO, USA). Glucose was supplied from Fluka (Buchs, Switzerland). MWCNTs (outer diameter <8 nm and length 10–30 μm) were obtained from Cheap Tubes Inc. (Brattleboro, USA). Graphene solution (DRP-GPHSOL) (2 mg/mL) was obtained from Dropsense (Llanera, Spain). High purity nitrogen gas was used for deaeration. All other chemicals were of analytical grade and used without further purification. Deionized water was used for preparation of buffer and standard solutions.

Apparatus and measurements

All electrochemical studies were performed using IVIUM electrochemical analyzer (Ivium Technologies, Netherlands). The electrochemical measurements were based on a conventional three-electrode system with a Ag/AgCl electrode (BAS MF 2052) as the reference electrode, a platinum wire electrode (BAS MW 1034) as the counter electrode, and the modified glassy carbon electrode (GCE, 3 mm diameter) as the working electrode. Scanning electron microscopy (SEM) images were obtained by using Carl Zeiss AG, EVO® 50 Series. The pH values of the testing solutions were measured with ORION Model 720A pH/ion meter and ORION combined pH electrode (Thermo Scientific, USA). The cyclic voltammograms of GCE and modified electrodes were recorded between (−1.00)V–(+1.00)V in the presence of 5 mM $K_3[(Fe(CN)_6]$, 5 mM $K_4[(Fe(CN)_6]$, and 0.1 M KCl. All measurements were carried out in a thermostated cell at 37 °C, containing 0.05 M phosphate buffer solution (PBS pH 7.5) under stirring at an applied potential of +0.70 V.

Biosensor preparation

The fabrication of Co_3O_4/MWCNTs/CS modified galactose biosensor was based on a simple method developed by our group [35]. Prior to coating, GCEs were polished with 0.05 μm alumina slurry, rinsed with deionized water, and sonicated in ethanol and double-distillated water for 5 min, respectively. Then, 0.025 g of CS was dissolved in 5.0 mL of acetate buffer solution (0.10 M and pH of 5.0) via magnetic stirring at room temperature for 4 h. Co_3O_4 nanoparticles and MWCNTs were dispersed into chitosan solution by stirring at room temperature and the resulting mixture was ultrasonicated for 4 h, until a homogenous black dispersion containing 1 mg/mL MWCNTs and 1 mg/mL Co_3O_4 nanoparticles was obtained. Furthermore, 10 μL of Co_3O_4/MWCNTs/CS solution was cast onto the pre-cleaned surface of GCE and dried at room temperature to construct the carbon nanotube-modified electrode. Graphene-modified biosensor was prepared using the following routes: (1) 5 μL of 2 mg/mL GR solution was cast onto the pre-cleaned surface of GCE and dried at room temperature. Co_3O_4 nanoparticles were dispersed in CS solution with 4 h of ultrasonication to achieve a 1 mg/mL concentration (Co_3O_4/CS). Five microliters of Co_3O_4/CS solution was cast onto the GR-coated GCE and dried at room temperature.

(2) Five microliters of 2 mg/mL GR solution was mixed with 5 μL of CS solution containing 1 mg/mL Co_3O_4, and the resulting mixture was ultrasonicated for 4 h. This homogenous mixture was dropped onto the surface of GCE and dried at room temperature to construct Co_3O_4/GR/CS/GCE. Then, 10 μL of GaOx solution (0.75 U/μL) was then cast on the surface of the GR and MWCNTs-modified electrodes. After being dried in refrigerator at 4 °C, GaOx/Co_3O_4/MWCNTs/CS/GCE, GaOx/Co_3O_4/CS/GR/GCE(1), and GaOx/Co_3O_4/GR/CS/GCE(2) were treated with 2.5 % glutaraldehyde vapour for 15 min for the crosslinking of the enzymes. The biosensors were fully washed with ultrapure water and dried in air. Then, 7.5 μL of nafion solution (0.5 %) was drop-coated on the enzyme electrode in order to prevent enzyme leakage. The as-prepared galactose biosensors were stored at 4 °C in a refrigerator when not in use. The stepwise fabrication processes of the modified electrodes are shown in Scheme 1.

Results and discussion

Morphologies and electrochemical characteristics of modified electrodes

The surface morphology of modified GCE was investigated by SEM. Figure 1 presents the SEM images of (a) Co_3O_4/MWCNTs/CS, (b) GaOx/Co_3O_4/MWCNTs/CS, (c) GR, (d) Co_3O_4/ CS/GR, and (e) GaOx/Co_3O_4/CS/GR modified GCE surfaces.

In Fig. 1, image a shows that the MWCNTs and Co_3O_4 nanoparticles are uniformly dispersed in the chitosan network. The porous morphology of the resulting film is suitable for the immobilization of enzymes. The surface morphology of GR/GCE (image c), shows wrinkled shapes of graphene. SEM image shown in Fig. 1d further confirms the effective distribution of Co_3O_4 nanoparticles on GR. The surfaces of GaOx/MWCNTs/Co_3O_4/CS/GCE (image b) and GaOx/Co_3O_4/CS/GR/GCE (image e) show globular structures on the composites indicating that enzymes were successfully immobilized on the surface of the nanocomposites. The SEM images of MWCNTs/CS/GCE and Co_3O_4/CS/GCE was reported before by our group [35].

Electrochemical properties of the modified electrodes were characterized by CV measurements. Figure 2 shows the CVs of bare GCE and modified electrodes. CVs were performed in 0.10 M KCl solution containing 5 mM potassium ferro/ferricyanide as a model reversible redox couple. A pair of redox peaks corresponding to the redox reaction of ferro/ferricyanide was observed at the bare GCE (curve a). When the electrode was further modified with graphene (curve b) or MWCNTs/CS film (curve c), the peak currents both increased while the peak-to-peak separation decreased, which indicated that the introducing of MWCNTs or graphene can increase the active surface area of electrode and facile the electron transfer between redox probe and electrode. Compared to GR/GCE, the electrode modified with MWCNTs had larger peak currents, mainly due to the higher specific area of MWCNTs. The magnitude of current response for Co_3O_4/MWCNTs/CS/GCE (curve d) and Co_3O_4/CS/GR/GCE (curve e) increases in comparison to that of bare GCE, GR/GCE, and MWCNTs/CS/GCE. This may be attributed to the presence of Co_3O_4 nanoparticles with increased electron mobility at the electrode surface resulting in enhanced electron transfer [4, 5] and synergistic action of the Co_3O_4 nanoparticles with graphene [36] or

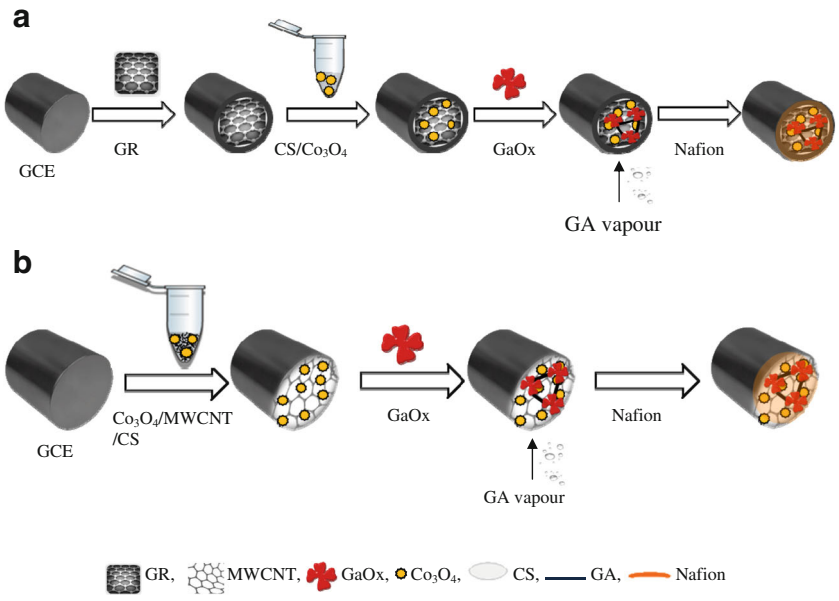

Scheme 1 Stepwise fabrication processes of **a** GR and **b** MWCNTs-modified electrodes

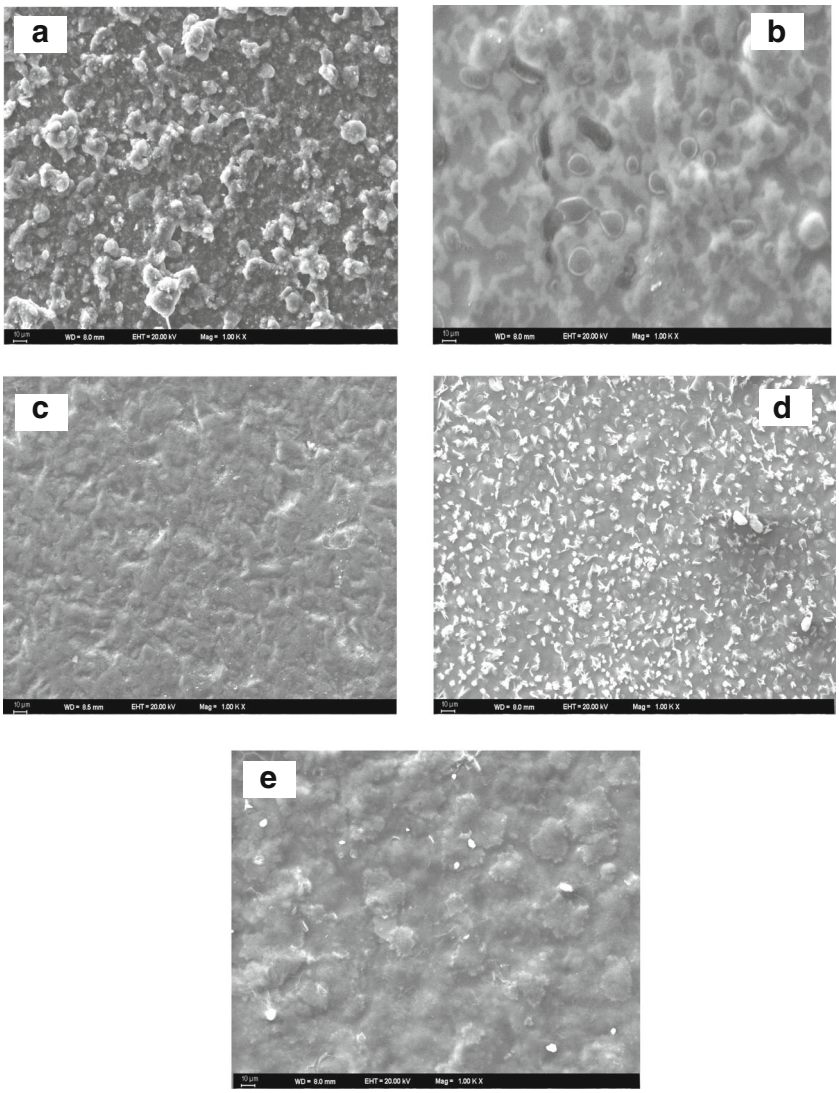

Fig. 1 SEM images of **a** MWCNTs/Co_3O_4/CS/GCE, **b** GaOx/MWCNTs/Co_3O_4/CS/GCE, **c** GR/GCE, **d** Co_3O_4/CS/GR/GCE, and **e** GaOx/Co_3O_4/CS/GR/GCE

MWCNTs [35]. Moreover, the peak currents obtained with Co_3O_4/MWCNTs/CS/GCE and Co_3O_4/CS/GR/GCE were close to each other. CVs of Co_3O_4/CS/GR/GCE(1) and Co_3O_4/GR/CS/GCE(2) were recorded to compare different electrode fabrication methods for graphene-based electrodes. The peak current obtained with Co_3O_4/GR/CS/GCE(2) was lower than that of the Co_3O_4/CS/GR/GCE(1). Thus, Co_3O_4/GR/CS/GCE(2) was used for further studies.

CV was performed on the GR/GCE, MWCNTs/CS/GCE, Co_3O_4/MWCNTs/CS/GCE, and Co_3O_4/CS/GR/GCE at varying scan rates (10–300 mV s^{-1}) in 0.1 M KCl containing 5 mM potassium ferro/ferricyanide. The CV of Co_3O_4/MWCNTs/CS/GCE is shown in Fig. 2b. The cathodic (ip_c) and (ip_a) anodic peak current plotted against the square root of the scan rate was linear (Fig. 2 inset), confirming the reversible redox reaction of the $Fe(CN)_6^{3-/4-}$ on the modified electrodes. The effective surface area of the GCE, GR/GCE, MWCNTs/CS/GCE, Co_3O_4/MWCNTs/CS/GCE, and Co_3O_4/CS/GR/GCE was estimated according to the Randles-Sevcik equation and referred to as "Eq. (1)" [37]:

$$I_p = 2.69 \times 10^{-5} * n^{3/2} A D^{1/2} v^{1/2} C \quad (1)$$

where *Ip* is the peak current of the redox reaction of $[Fe(CN)_6]^{3-/4-}$ (A), n is the number of electrons participating in the redox reaction (1), A is the effective surface area (cm^2), D is the diffusion coefficient (7.6×10^{-6} cm^2 s^{-1} at 25 °C), v is the scan rate (V s^{-1}), and C is the concentration of $[Fe(CN)_6]^{3-/4-}$ (5 mM). The effective surface area of the GCE, GR/GCE, MWCNTs/CS/GCE, Co_3O_4/CS/GCE, Co_3O_4/MWCNTs/CS/GCE, and Co_3O_4/CS/GR/GCE was 0.071, 0.099, 0.132, 0.106, 0.188, and 0.198 cm^2, respectively. In comparison with the bare GCE, the effective surface area of the GR, Co_3O_4/CS, and MWCNTs/CS modified electrodes was increased by about 1.3, 1.49, and 1.85 times, respectively. These results

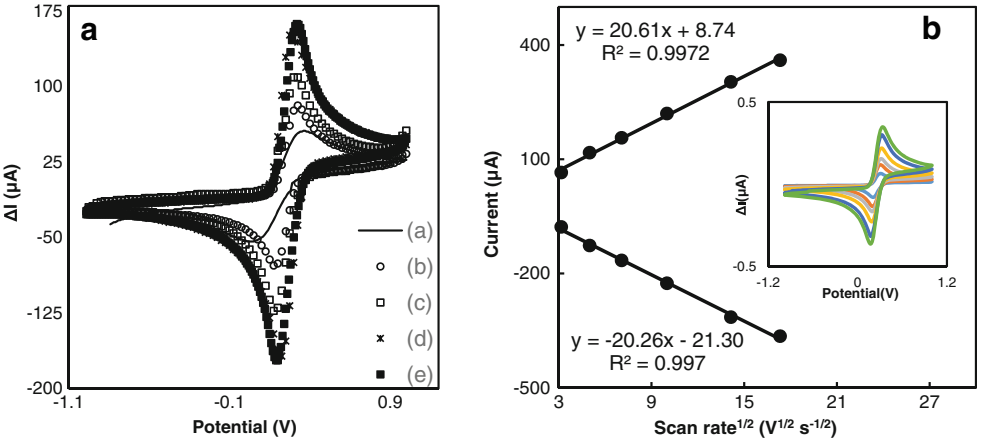

Fig. 2 **A** Cyclic voltammograms of **a** GCE, **b** GR/GCE, **c** MWCNTs/CS/GCE, **d** Co_3O_4/CS/MWCNTs/GCE, and **e** Co_3O_4/CS/GR/GCE at 50 mV s^{-1}. **B** Cyclic voltammograms of the Co_3O_4/MWCNTs/CS/GCE at scan rates of 10, 20, 50, 75, 100, 200, and 300 mV s^{-1} in a 0.1 M KCl solution containing 5 mM $Fe(CN)_6^{3-/4-}$ Inset: Peak currents as a function of scan rate for the determination of the effective working surface area

were expected, as MWCNTs, Co_3O_4 nanoparticles and GR facilitate enhanced electron transfer for the redox process of $Fe(CN)_6^{3-/4-}$ [4, 5, 35], thus increasing the effective surface area available for signal transduction. The effective surface areas of the Co_3O_4/MWCNTs/CS/GCE and Co_3O_4/CS/GR/GCE are higher than that of GR/GCE and MWCNTs/CS/GCE electrodes, suggesting that Co_3O_4 nanoparticle modification leads to a higher electroactive area.

Optimization of experimental parameters

GaOx catalyzes the formation of H_2O_2 from galactose and enzymatically produced H_2O_2 can be detected electrochemically by its oxidation. Thus, the electrochemical oxidation of H_2O_2 at bare GCE, MWCNTs/CS/GCE, Co_3O_4/MWCNTs/CS/GCE, GR/GCE, and Co_3O_4/CS/GR/GCE electrodes was investigated by plotting calibration graphs. H_2O_2 sensitivity of the Co_3O_4/MWCNTs/CS/GCE (16.01 μA/mM cm^2) and Co_3O_4/CS/GR/GCE (9.03 μA/mM cm^2) were found to be much higher than that of bare GCE (1.12 μA/mM cm^2), MWCNTs/CS/GCE (16.13 μA/mM cm^2), and GR/GCE (9.89 μA/mM cm^2) at +0.70 V. It can be concluded that both Co_3O_4/MWCNTs/CS/GCE and Co_3O_4/CS/GR/GCE promotes the electrooxidation of H_2O_2. Therefore, these electrodes can be used as effective platforms for the construction of galactose biosensors.

GaOx was immobilized onto Co_3O_4/MWCNTs/CS/GCE and Co_3O_4/CS/GR/GCE by crosslinking with glutaraldehyde to construct the galactose biosensors. To investigate the effect of the enzyme amount on the biosensor response, different enzyme amounts were used in the biosensor construction. For this purpose, enzyme electrodes containing GaOx between 3 and 12 U were prepared and the amperometric responses of the biosensors in 0.05 mol L^{-1} phosphate buffer solution containing 0.2 mM galactose were measured. The current difference increased from 3 to 7.5 U and then decreased afterwards with both biosensors. As the maximum current difference was achieved with 7.5 U, this enzyme amount was used for further experiments. The increase in the amount of GaOx on the enzyme electrodes resulted in the increase in the active site of the enzyme electrodes, and the sensitivity of the biosensors hence increased. The immobilization of a higher amount of GaOx did not improve biosensor response. The current decrease at higher enzyme loadings may be attributed to the limited diffusion of the substrate to the matrix due to the large amount of immobilized enzyme [38].

The applied potential strongly affects the amperometric response of a biosensor. We have investigated the effect of the applied potential on the amperometric response of the purposed biosensors to galactose. The response of GaOx/Co_3O_4/MWCNTs/CS/GCE and GaOx/Co_3O_4/CS/GR/GCE to constant galactose concentration (0.2 mM) was determined at different working potentials between (+0.50) and (+0.70) V. The maximum current difference was obtained at +0.70 V. Therefore, +0.70 V was selected for the amperometric experiments.

The electron transfer mechanism of the presented biosensors is based on the formation of H_2O_2 from galactose by GaOx enzyme immobilized in the Co_3O_4/MWCNTs/CS and Co_3O_4/CS/GR nanocomposites and its oxidation at an applied potential of +0.70 V and referred to as "reaction (2) and (3)".

$$\text{Galactose} + O_2 \xrightarrow{\text{GaOx}} \text{Galactonic acid} + H_2O_2 \quad (2)$$

$$H_2O_2 \xrightarrow{+0.70\ \text{V}} 2H^+ + 2e^- + O_2 \quad (3)$$

The response current of the biosensors are directly proportional to galactose concentration.

The pH value of the electrolyte is important for the performance of the biosensor because the activity of the enzyme is affected greatly by pH [39]. Figure 3a shows the amperometric responses of GaOx/Co_3O_4/MWCNTs/CS/GCE and GaOx/Co_3O_4/CS/GR/GCE at different pH values with the

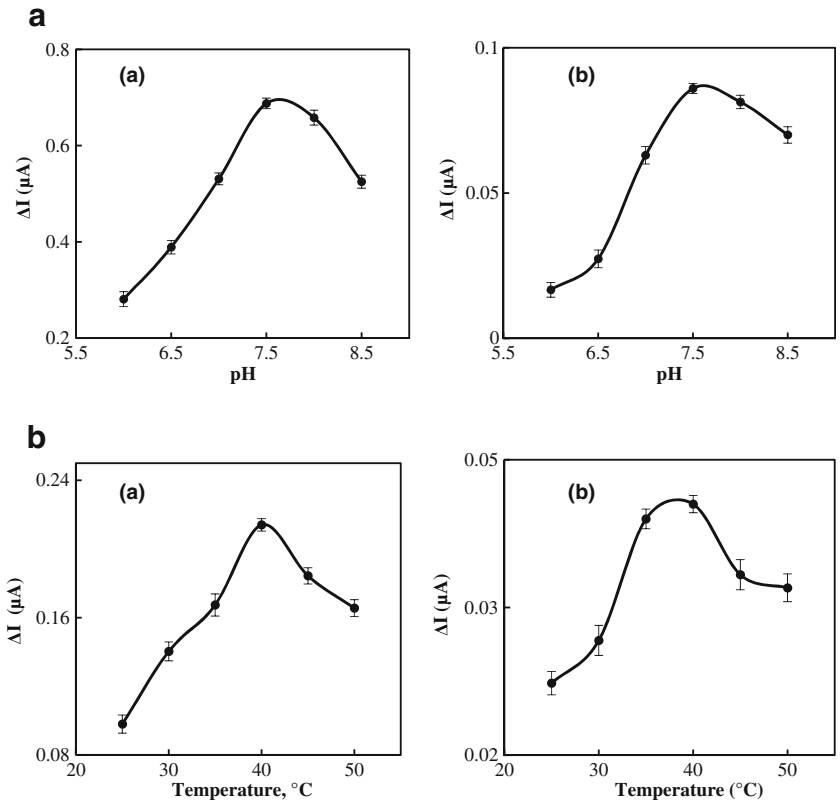

Fig. 3 The effect of buffer pH (**A**) and temperature (**B**) on the responses of **a** GaOx/MWCNTs/Co_3O_4/CS/GCE and **b** GaOx/Co_3O_4/CS/GR/GCE (0.05 M PBS, +0.70 V)

presence of the same concentration of galactose. It can be seen that the response current increases with pH value ranging from 6.0 to 7.5, after reaching its maximum at pH 7.5, then it decreases as pH increases further. In order to achieve the maximum sensitivity, pH 7.5 PBS was selected as the electrolyte in subsequent experiments. This optimum value is also compatible with the pH range (7.0–7.3) reported for the free GaOx [30, 40, 41]. This study indicates that the immobilization procedure has no significant effect on the optimum pH of GaOx. A comparison of the optimum pH with the previously reported values is presented in Table 1.

Temperature has a great effect on enzyme activity, and it is important to investigate the temperature dependence of the response of the biosensor. The temperature influence on the responses of GaOx/Co_3O_4/MWCNTs/CS/GCE and GaOx/Co_3O_4/CS/GR/GCE was tested between 25 and 50 °C at pH 7.5 (Fig. 3b). With an increasing temperature from 25 to 40 °C, the activity of immobilized enzymes increased, leading to the increasing amperometric response. When the temperature was higher than 40 °C, the amperometric response decreased. The decrease after 40 °C is thought to be caused by the denaturation of the enzyme. This result is very convenient with the results reported in the literature for galactose biosensors based on Langmuir–Blodgett film [18], polyacrylonitrile thin film-modified platin electrode [42], and single-walled carbon nanotubes-modified GCE [26]. Although best current response obtained at 40 °C galactose measurements were performed at body temperature (37 °C) at which the response was about 90 % of the maximum biosensor response. This value is also convenient with the optimum temperature (32 °C) of the free GaOx [29, 30].

Analytical performance of the biosensors

Figure 4 shows the calibration curves and typical current–time responses (inset) at (a) GaOx/Co_3O_4/MWCNTs/CS/GCE and (b) GaOx/Co_3O_4/CS/GR/GCE for successive addition of galactose. The linear response range of the GaOx/Co_3O_4/MWCNTs/CS/GCE biosensor to galactose concentration was from 9.0×10^{-6} to 1.0×10^{-3} M with a correlation coefficient of 0.9973. The detection limit based on a signal-to-noise ratio (*S*/*N*) of 3 was estimated to be 2.2×10^{-6} M, which is lower than that of laponite clay film-modified Pt electrode (1.0×10^{-6} M) [14], ZnO nanorods-modified glass substrate (1.0×10^{-3} M) [16], and poly(glycidylmethacrylate-co-vinylferrocene)-modified Pt electrode (1.0×10^{-4} M) [43]. The sensitivity of the GaOx/Co_3O_4/MWCNTs/CS/GCE was estimated to be 10.39 μA/mM cm^2. GaOx/Co_3O_4/CS/GR/GCE showed linear responses to galactose at concentrations of 9.0×10^{-6}–6.0×10^{-4} M with a correlation coefficient of 0.9968. The detection limit of the biosensor was 3.0×10^{-6} M (*S*/*N* = 3), higher than that of GaOx/Co_3O_4/MWCNTs/CS/GCE. This detection limit is lower than that of cobalt

Table 1 Characteristics of various amperometric galactose biosensors

Electrode	Working potential, V	Detection limit, M	Linear range, M	Sensitivity	Response time, s	K_m	pH/Temperature °C	Reference
Cobalt phthalocyanine modified screen-printed carbon electrode	+0.50 vs. Ag/ AgCl	2.0×10^{-5}	1.0×10^{-4}–25×10^{-3}	0.63 μA/mM	30	–	7.0/35	[17]
Poly(*N*-glycidylpyrrole-co-pyrrole) film-modified gold electrode	+0.70 vs. Ag/ AgCl	25×10^{-6}	2.0×10^{-3}–16×10^{-3}	1.75 μA/mM	5	14.7 mM	7.5/–	[27]
Laponite clay film-coated platin electrode	+0.60 vs. Ag/ AgCl	1.0×10^{-6}	1.0×10^{-6}–1.6×10^{-3}	85 mA/M cm^2	5	–	7.0/25	[14]
Poly(glycidylmethacrylate-co-vinylferrocene)-modified platin electrode	+0.35 vs. Ag/ AgCl	1.0×10^{-4}	2.0×10^{-3}–2.0×10^{-2}	23 nA/mM cm^2	5	16 mM	6.5/35	[43]
Conducting polymer tubules-modified ITO electrode	+0.60 vs. Ag/ AgCl	1.0×10^{-5}	1.0×10^{-4}–1.0×10^{-3}	6.37 mA/mM cm^2	30–40	–	–	[19]
Single-walled carbon nanotubes-modified GCE	–0.40 V vs. Ag/ AgCl	25×10^{-6}	Up to 1.0×10^{-3}	1126 nA/mM	150 injection/ hour	–	7.4/–	[26]
Polypyrrole, polyanion/poly(ethylene glycol)/enzyme conjugate dopant modified	+0.40 V vs. Ag/ AgCl	–	0–24×10^{-3}	106 nA/mM cm^2	<40	43 mM	7.4/37	[44]
Polyacrylonitrile thin film-modified platin electrode	+0.50 vs. SCE	–	2.0×10^{-5} – 1.6×10^{-3}	–	–	12.15 mM	7.1/40	[42]
Eggshell membrane-modified oxygen electrode	–	–	1.0×10^{-4}–8.5×10^{-3}	–	100	–	7.0/RT	[45]
Chitosan and prussian blue-modified platin electrode	+0.05 V vs.	6.0×10^{-5}	1.0×10^{-4}–6.0×10^{-3}	49 nA/mM	42–60	–	6.8/25	Wang et al. [47]
Polyvinylferrocenium-modified platin electrode	+0.70 vs. SCE	–	Up to 4.0×10^{-2}	–	30–40	21.7 mM	13/25	[46]
Co_3O_4 nanoparticles and graphene-modified GCE	+0.70 vs. Ag/AgCl	3.0×10^{-6}	9.0×10^{-6}–6.0×10^{-4}	0.43 μA/mM or 6.60 μA/ mM cm^2	15	1.16 mM	7.5/37	This work
Co_3O_4 nanoparticles and MWCNTs modified GCE	+0.70 vs. Ag/AgCl	9.0×10^{-7}	9.0×10^{-6} – 1.0×10^{-3}	0.79 μA/mM or 10.39 μA/ mM cm^2	20	0.66 mM	7.5/37	This work

RT room temperature

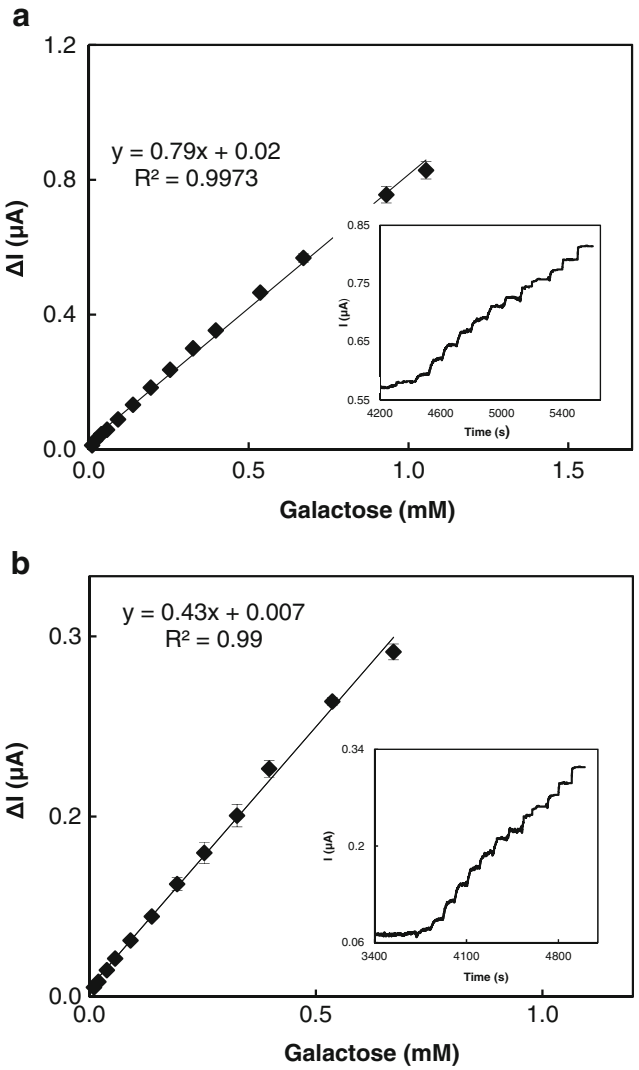

Fig. 4 Calibration curves of the **a** GaOx/MWCNTs/Co_3O_4/CS/GCE and **b** GaOx/Co_3O_4/CS/GR/GCE Inset: Typical current–time response of the on successive injection of galactose into a stirred solution of 0.05 M PBS (pH 7.5) at applied potential +0.70 V at 37 °C

phthalocyanine-modified screen-printed electrode (2.0×10^{-5} M) [17] and chitosan-prussian blue-modified Pt electrode (6.0×10^{-5} M) [47] but comparable to Clark-type microbial biosensor (2.0×10^{-6} M) [48]. The sensitivity of the GaOx/Co_3O_4/CS/GR/GCE was 6.60 μA/mM cm^2. The sensitivity of the GaOx/Co_3O_4/MWCNTs/CS/GCE was about 1.6-fold higher than that of GaOx/Co_3O_4/CS/GR/GCE. GaOx/Co_3O_4/MWCNTs/CS/GCE biosensors reached 95 % of the steady-state current within 20 s while this is 15 s with its graphene counterpart.

The effective surface areas of the Co_3O_4/MWCNTs/CS/GCE (0.188 cm^2) and Co_3O_4/CS/GR/GCE (0.198 cm^2) were close to each other. However, the sensitivity of the GaOx/Co_3O_4/MWCNTs/CS/GCE was found to be higher than its graphene counterpart. This may be attributed to the following reasons: (i) metal impurities in MWCNTs such as

iron oxide and copper oxide resulting from the fabrication process of the MWCNTs were reported in the literature [49, 50]. The presence of these metal impurities embedded inside the MWCNTs that act like catalytic centers may cause the electrocatalysis which is responsible from the increased sensitivity of the MWCNTs-based galactose biosensor. (ii) It was reported that the modification of chitosan by bifunctional cross-linking reagent glutaraldehyde is widely used to form films, microcapsules, or hydrogels that are insoluble in water and immobilize enzymes or other proteins in their structure. In this type of immobilization, glutaraldehyde establishes intermolecular cross-links with amino groups of the enzyme and those of this polymer [51, 52]. The amount of chitosan used in the preparation of GaOx/Co_3O_4/MWCNTs/CS/GCE is higher than its graphene counterpart. This higher chitosan amount may result in higher enzyme loading which is responsible for the enhanced sensitivity.

The apparent Michaelis–Menten constant (K_M^{app}), a reflection of enzymatic affinity, can be calculated by use of the Lineweaver–Burk equation, and this equation is given as "Eq. (4)":

$$\frac{1}{i_{ss}} = \frac{1}{i_{\max}} + \frac{K_M{}^{app}}{i_{\max}} x \frac{1}{C} \tag{4}$$

where i_{ss} is the steady-state current after addition of substrate, i_{max} is the maximum current measured under saturated substrate conditions, and C is the bulk concentration of the substrate [53]. The lower K_M^{app} value means that the immobilized galactose oxidase possesses higher affinity to galactose. The K_M^{app} value was calculated to be 0.66 mM for GaOx/Co_3O_4/MWCNTs/CS/GCE and 1.16 mM for GaOx/Co_3O_4/CS/GR/GCE which are lower than that for most previous galactose biosensors [41–46] indicating increased affinity of galactose oxidase toward galactose after immobilization on Co_3O_4/CS/GR/GCE and Co_3O_4/MWCNTs/CS/GCE surfaces.

The repeatability, reproducibility, and stability of our proposed biosensors have also been studied. Five calibration curves were plotted by the use of the same electrode sequentially. The relative standard deviation (RSD) of the sensitivities was 3.6 % for GaOx/Co_3O_4/MWCNTs/CS/GCE and 1.7 % for GaOx/Co_3O_4/CS/GR/GCE. Five electrodes were prepared utilizing the same method to check the reproducibility of the biosensor. To detect the same concentration range of galactose, the result revealed a RSD of 3.2, and 2.3 % for GaOx/Co_3O_4/MWCNTs/CS/GCE and GaOx/Co_3O_4/CS/GR/GCE, respectively. This demonstrated the excellent repeatability and reliable reproducibility of the biosensors. The long-term stability of our fabricated biosensors was investigated by examining their current response during storage in a refrigerator at 4 °C. After storage of 1 month, GaOx/Co_3O_4/MWCNTs/CS/GCE lost 40 % of its original sensitivity and GaOx/Co_3O_4/CS/GR/GCE lost 55 % of its original sensitivity.

In order to assess the analytical performance of the proposed biosensors, the characteristics in terms of linear working range, detection limit, stability, and K_m were compared with earlier galactose biosensors (Table 1). It can be found that the GaOx/Co_3O_4/MWCNTs/CS/GCE and GaOx/Co_3O_4/CS/GR/GCE biosensors exhibited a wider linear range and very low detection limit in the detection of galactose. Moreover, the presented biosensors have favorable analytical performance which might be attributed to the excellent conductivity of Co_3O_4/MWCNTs/CS and Co_3O_4/CS/GR nanocomposites.

The analytical characteristic of presented biosensors was also compared with some other techniques developed for galactose determination. Chávez-Servín et al. [54] reported a high-performance liquid chromatography (HPLC) method with refractive index (RI) detection for the determination of galactose. The linear working range of this method was reported as 2.8×10^{-3}–5.0×10^{-2} M and detection limit was reported as 3.3×10^{-4} M. Ning et al. [55] measured plasma galactose concentration by gas chromatography/mass spectrometry. The method was reported to be linear from 1×10^{-7} to 1×10^{-5} M for galactose with a detection limit of 1×10^{-7} M. Henderson et al. [24] developed a fluorometric method for galactose determination in blood or plasma and the linear working range of this method was found as 1.1×10^{-5}–5×10^{-5} M. A spectrophotometric method was reported by Kurtz et al. [22] for enzymatic determination of galactose with a working range 8×10^{-5}–2×10^{-3} M. These methods generally show higher detection limits and narrower linear working ranges for galactose than the electrochemical biosensors. Moreover, such methods of detection are often complicated, expensive, time-consuming, and require experienced personnel. The presented biosensors show better characteristics (Table 1) than the other methods.

The effects of several possible interfering substances on the GaOx/Co_3O_4/MWCNTs/CS/GCE and GaOx/Co_3O_4/CS/GR/GCE were investigated at +0.70 V versus Ag/AgCl in pH 7.5 phosphate buffer. Ascorbic acid, urea, glucose, uric acid, creatinine, aspartic acid, and methionine were used to evaluate the selectivity of the purposed biosensors. Amperometric responses were obtained by injection of 0.01 mM galactose and interfering species of different concentration. The concentrations of the interfering substances and galactose were 100-fold lower than their physiological concentrations [56] since diluted serum samples were used for the real sample analysis. The interference was determined as the percentage of the current signal, obtained for detecting 0.01 mM galactose, which was contributed by the addition of a particular interfering substance. The interference (%) at the GaOx/Co_3O_4/MWCNTs/CS/GCE and GaOx/Co_3O_4/CS/GR/GCE to the addition of interfering substances in 0.05 M phosphate buffer solution (pH 7.5) are shown in Table 2. Creatinine, urea, methionine, and aspartic acid did not cause any considerable interference

Table 2 Results of interference experiments on the current response of 0.01 mM galactose on (a) GaOx/MWCNTs/Co_3O_4/CS/GCE and (b) GaOx/Co_3O_4/CS/GR/GCE ($n = 3$)

Interference substances	Physiological concentration in serum (mM)	Concentration[a] (mM)	Interference (%) (a)	Interference (%) (b)
Glucose	4	0.04	1	3
Ascorbic acid	0.2	0.002	1	2
Creatinine	0.1	0.001	–	–
Urea	0.8	0.008	–	–
Methionine	5×10^{-5}	5×10^{-7}	–	–
Aspartic acid	0.01	0.0001	–	–
Uric acid	0.2	0.002	20	27

[a] Concentrations of interference substances in aqueous media

to the detection of 0.01 mM galactose by GaOx/Co_3O_4/MWCNTs/CS/GCE and GaOx/Co_3O_4/CS/GR/GCE while ascorbic acid and glucose caused less than 4 % interference. However, uric acid caused 20 and 27 % interference on the responses of GaOx/Co_3O_4/MWCNTs/CS/GCE and GaOx/Co_3O_4/CS/GR/GCE, respectively. This effect can be attributed to the high working potential. The serum samples of patients with galactosemia should be diluted to obtain reliable results with biosensors due to elevated levels of galactose. The interference effect of uric acid can be minimized by sample dilution or using standard addition method. It can be concluded that the GaOx/Co_3O_4/MWCNTs/CS modified electrode exhibited slightly better selectivity than the GaOx/Co_3O_4/CS/GR modified electrode.

Analysis of real samples

The level of galactose in normal human plasma samples is too low to be detected. However, it would be determinable for diagnosing galactosemia in infants with an abnormal galactose level. First human serum sample from healthy individuals was analyzed with chromatographic method to investigate the galactose level. The results of this method demonstrated that the galactose level in the analyzed serum sample was below the detection limit of the method. Therefore, the serum sample was spiked with three different concentrations of standard galactose solution and these spiked serum samples were assayed to demonstrate the practical use of GaOx/Co_3O_4/MWCNTs/CS/GCE and GaOx/Co_3O_4/CS/GR/GCE. The spiked serum sample was diluted 250 times with 0.05 M pH 7.5 phosphate buffer without any other pretreatment process before its analyses with the presented biosensors. Standard addition method was used to determine the galactose content in spiked serum sample. In this method, additions of standard galactose solution were made to each spiked serum sample, and a multiple addition calibration curve was obtained. It was shown that the calibration curve is linear and galactose concentration in spiked serum sample was calculated from this

Table 3 The result of the recovery studies of standard additions to human serum samples obtained with two galactose biosensors

GaOx/Co_3O_4/MWCNTs/CS/GCE			GaOx/Co_3O_4/GR/CS/GCE		
Galactose added (mg L^{-1})[a]	Galactose found (mg L^{-1})	Recovery, %	Galactose added (mg L^{-1})[a]	Galactose found (mg L^{-1})	Recovery, %
14.16	14.28 ± 0.16	100.9 ± 1.1	14.16	14.20 ± 0.01	100.3 ± 0.1
34.98	34.94 ± 0.69	99.9 ± 2.0	34.98	34.33 ± 0.27	98.1 ± 0.8
58.67	57.39 ± 1.96	97.8 ± 3.3	58.67	58.75 ± 2.30	100.1 ± 3.9
84.98	78.98 ± 1.40	93.3 ± 1.6	84.98	81.02 ± 3.30	93.3 ± 3.9
$R\%_{mean}$: 98.0 ± 3.3			$R\%_{mean}$: 98.0 ± 3.2		

Galactose analysis in human serum sample was performed by METU Central Laboratory, Molecular Biology-Biotechnology Research and Development Center, Chromatography and Fermentation Laboratory, Ankara, Turkey, with VARIAN ProStar HPLC via VARIAN Metacarb 87H Processing Method (MetaCarb 87H Column, 300 × 7,8 mm; PN:A5210, VARIAN). The galactose level was found below the detection limit of the method

[a] The amount of standard additions were made according to the linear working ranges of the biosensors. Results are the mean value of three measurements ($n = 3$)

calibration curve. The related data are given in Table 3. Table shows that a mean recovery value of about 100 % was obtained ($N=3$) and $ts/\sqrt{N}$ was about 3 % for the spiked serum samples with both biosensors. From these recovery values, it is concluded that proposed biosensors can be used for the determination of galactose in serum samples with a good recovery.

Conclusions

The Co_3O_4/CS/GR and Co_3O_4/MWCNTs/CS nanocomposites had been successfully coated onto GCE to fabricate the presented galactose biosensors. GaOx was immobilized onto the composite films by crosslinking. Because of the synergistic effects between the MWCNTs or GR and Co_3O_4 nanoparticles, both biosensors showed good performance in the merits of low detection limit, good repeatability, wide linear working range, and short response time. The results of the presented study indicated that the GaOx/Co_3O_4/MWCNTs/CS modified electrode exhibited higher sensitivity, lower detection limit, wider linear working range, lower K_M^{app}, slightly better selectivity, and higher storage stability for galactose detection than the GaOx/Co_3O_4/CS/GR modified electrode. It can be concluded that Co_3O_4/CS/GR and Co_3O_4/MWCNTs/CS nanocomposites have great potential in the fabrication of biosensors for the detection of different species.

Acknowledgments We gratefully acknowledge the financial support of Ankara University Research Fund (Project No: 13L4240002) and a scholarship for B.DALKIRAN of The Scientific and Technological Research Council of Turkey.

Compliance with ethical standards

Conflict of interest The authors declare that they have no conflict of interest.

References

1. Yang W, Ratinac KR, Ringer SP, Thordarson P, Gooding JJ, Braet F. Carbon nanomaterials in biosensors: should you use nanotubes or graphene? Angew Chem Int Ed. 2010;49:2114–38.
2. Wang J. Electrochemical biosensing based on noble metal nanoparticles. Microchim Acta. 2012;177:245–70.
3. Terzi F, Pelliciari J, Zanardi C, Pigani L, Viinikanoja A, Lukkari J, et al. Graphene-modified electrode. Determination of hydrogen peroxide at high concentrations. Anal Bioanal Chem. 2013;405:3579–86.
4. Pérez-López B, Merkoci A. Carbon nanotubes and graphene in analytical sciences. Microchim Acta. 2012;179(1-2):1–16.
5. Kuila T, Bose S, Khanra P, Mishra AK, Kim NH, Lee JH. Recent advances in graphene-based biosensors. Biosens Bioelectron. 2011;26(12):4637–48.
6. Salimi A, Hallaj R, Soltanian S. Fabrication of a sensitive cholesterol biosensor based on cobalt-oxide nanostructures electrodeposited onto glassy carbon electrode. Electroanalysis. 2009;21:2693–700.
7. Devi R, Yadav S, Nehra R, Yadav S, Pundir CS. Electrochemical biosensor based on gold coated iron nanoparticles/chitosan composite bound xanthine oxidase for detection of xanthine in fish meat. J Food Eng. 2013;115:207–14.
8. Jang HD, Kim SK, Chang H, Roh KM, Choi JW, Huang J. A glucose biosensor based on TiO_2–graphene composite. Biosens Bioelectron. 2012;38(1):184–8.
9. Zhou K, Zhu Y, Yang X, Li C. Preparation and application of mediator-free H_2O_2 biosensors of graphene-Fe_3O_4 composites. Electroanalysis. 2011;23(4):862–9.
10. Wang G, Tan X, Zhou Q, Liu Y, Wang M, Yang L. Synthesis of highly dispersed zinc oxide nanoparticles on carboxylic graphene for development a sensitive acetylcholinesterase biosensor. Sensors Actuators B Chem. 2014;190:730–6.
11. Teymourian H, Salimi A, Hallaj R. Low potential detection of NADH based on Fe_3O_4 nanoparticles/multiwalled carbon nanotubes composite: fabrication of integrated dehydrogenase-based lactate biosensor. Biosens Bioelectron. 2012;33(1):60–8.
12. Numnuam A, Thavarungkul P, Kanatharana P. An amperometric uric acid biosensor based on chitosan-carbon nanotubes electrospun nanofiber on silver nanoparticles. Anal Bioanal Chem. 2014;406:3763–72.
13. Kaçar C, Dalkiran B, Erden PE, Kilic E. An amperometric hydrogen peroxide biosensor based on Co_3O_4 nanoparticles and multiwalled carbon nanotube modified glassy carbon electrode. Appl Surf Sci. 2014;311:139–46.
14. Charmantray F, Touisni N, Hecquet L, Mousty C. Amperometric biosensor based on galactose oxidase immobilized in clay matrix. Electroanalysis. 2013;25(3):630–5.
15. Berry GT, Hunter JV, Wang Z, Dreha S, Mazur AD, Brooks G, et al. In vivo evidence of brain galactitol accumulation in an infant with galactosemia and encephalopathy. J Pediatr. 2001;138:260–2.
16. Khun K, Ibupoto ZH, Nur O, Willander M. Development of galactose biosensor based on functionalized ZnO nanorods with galactose oxidase journal of sensors volume. J Sens. 2012. doi:10.1155/2012/696247.
17. Kanyong P, Pemberton RM, Jackson SK, Hart JP. Development of an amperometric screen-printed galactose biosensor for serum analysis. Anal Biochem. 2013;435:114–9.
18. Sharma SK, Singhal R, Malhotra BD, Sehgal N, Kumar A. Langmuir–Blodgett film based biosensor for estimation of galactose in milk. Electrochim Acta. 2004;49:2479–85.
19. Lee KN, Lee Y, Son Y. Enhanced sensitivity of a galactose biosensor fabricated with a bundle of conducting polymer microtubules. Electroanalysis. 2010;23(9):2125–30.
20. Sharma SK, Singh SK, Sehgal N, Kumar A. Biostrip technique for detection of galactose in dairy foods. Food Chem. 2004;88:299–303.
21. Hansen SA. Thin-layer chromatographic method for the identification of mono-, di-and trisaccharides. J Chromatogr. 1975;107(1):224–6.
22. Kurtz KS, Crouch SR. Design and optimization of a flow-injection system for enzymatic determination of galactose. Anal Chim Acta. 1991;254(1):201–8.
23. Cataldi TRI, Angelotti M, Bianco G. Determination of mono-and disaccharides in milk and milk products by high-performance anion-exchange chromatography with pulsed amperometric detection. Anal Chim Acta. 2003;485:43–9.
24. Henderson JM, Fales FW. Continuous-flow fluorometry of low galactose concentrations in blood or plasma. Clin Chem. 1980;26(2):282–5.
25. Xie J, Chen C, Zhou Y, Fei J, Ding Y, Zhao J. A Galactose oxidase biosensor based on graphene composite film for the determination of galactose and dihydroxyacetone. Electroanalysis. 2015;27:1–7.

26. Tkac J, Whittaker JW, Ruzgas T. The use of single walled carbon nanotubes dispersed in a chitosan matrix for preparation of a galactose biosensor. Biosens Bioelectron. 2007;22(8):1820–4.
27. Şenel M, Bozgeyik İ, Çevik E, Abasıyanık MF. A novel amperometric galactose biosensor based on galactose oxidase-poly (N-glycidylpyrrole-co-pyrrole). Synth Met. 2011;161(5):440–4.
28. Whittaker MM, Ballou DP, Whittaker JW. Kinetic isotope effects as probes of the mechanism of galactose oxidase. Biochemistry. 1998;37(23):8426–36.
29. Tkac J, Gemeiner P, Šturdík E. Rapid and sensitive galactose oxidase-peroxidase biosensor for galactose detection with prolonged stability. Biotechnol Tech. 1999;13:931–6.
30. Szabo EE, Adanyi N, Varadi M. Application of biosensor for monitoring galactose content. Biosens Bioelectron. 1996;11(10):1051–8.
31. Kanyong P, Hughes G, Pemberton RM, Jackson SK, Hart JP. Amperometric screen-printed galactose biosensor for cell toxicity applications. Anal Lett. 2015;49(2):236–44.
32. Zheng D, Vashist SK, Dykas MM, Saha S, Al-Rubeaan K, Lam E, et al. Luong and fwu-shan sheu, graphene versus multi-walled carbon nanotubes for electrochemical glucose biosensing. Materials. 2013;6:1011–27.
33. You JM, Kim D, Jeon S. Electrocatalytic reduction of H_2O_2 by Pt nanoparticles covalently bonded to thiolated carbon nanostructures. Electrochim Acta. 2012;65:288–93.
34. Liu C, Alwarappan S, Chen Z, Kong X, Li CZ. Membraneless enzymatic biofuel cells based on graphene nanosheets. Biosens Bioelectron. 2010;25:1829–33.
35. Dalkiran B, Kacar C, Erden PE, Kilic E. Amperometric xanthine biosensors based on chitosan-Co_3O_4 multiwall carbon nanotube modified glassy carbon electrode. Sensors Actuators B Chem. 2014;200:83–91.
36. Dong XC, Hang X, Wang XW, Huang YX, Chan-Park MB, Zhang H, et al. 3D graphene–cobalt oxide electrode for high-performance supercapacitor and enzymeless glucose detection. ACS Nano. 2012;6(4):3206–13.
37. Welch CM, Banks CE, Simm AO, Compton RG. Silver nanoparticle assemblies supported on glassy-carbon electrodes for the electro-analytical detection of hydrogen peroxide. Anal Bioanal Chem. 2005;382(1):12–21.
38. Njagi J, Andreescu S. Stable enzyme biosensors based on chemically synthesized Au–polypyrrole nanocomposites. Biosens Bioelectron. 2007;23:168–75.
39. Zhiguo G, Shuping Y, Zaijun L, Xiulan S, Guangli W, Yinjun F, et al. An ultrasensitive hydrogen peroxide biosensor based on electrocatalytic synergy of graphene–gold nanocomposite, CdTe–CdS core–shell quantum dots and gold nanoparticles. Anal Chim Acta. 2011;701(1):75–80.
40. Vega FA, Núñez CG, Weigel B, Hitzmann B, Ricci JCD. On-line monitoring of galactoside conjugates and glycerol by flow injection analysis. Anal Chim Acta. 1998;373:57–62.
41. Jia NQ, Zhang ZR, Zhu JZ, Zhang GX. A Galactose biosensor based on the microfabricated thin film electrode. Anal Lett. 2003;36:2095–106.
42. Kan J, Chen C, Jing G. The galactose biosensor based on microporous polyacrylonitrile. Biocatal Biotransfor. 2005;23:439–44.
43. Çevik E, Senel M, Abasıyanık MF. Construction of biosensor for determination of galactose with galactose oxidase immobilized on polymeric mediator contains ferrocene. Curr Appl Phys. 2010;10:1313–6.
44. Sung WJ, Bae YH. Glucose oxidase, lactate oxidase, and galactose oxidase enzyme electrode based on polypyrrole with polyanion/PEG/enzyme conjugate dopan. Sensors Actuators B Chem. 2006;114:164–9.
45. Wen G, Zhang Y, Zhou Y, Shuang S, Dong C, Choi MMF. Biosensors for determination of galactose with galactose oxidase immobilized on eggshell membrane. Anal. Lett. 2005;38:1519–29.
46. Gülce H, Ataman I, Yildiz A. A new amperometric enzyme electrode for galactose determination. Enzym Microb Technol. 2002;30(1):41–4.
47. Wang Y, Zhu J, Zhu R, Zhu Z, Lai Z, Chen Z. Chitosan/Prussian blue-based biosensors. Meas Sci Technol. 2003;14:831–6.
48. Peteu SF, Emerson D, Worden RM. A Clark-type oxidase enzyme-based amperometric microbiosensor for sensing glucose, galactose, or choline. Biosens Bioelectron. 1996;11:1059–71.
49. Banks CE, Crossley A, Salter C, Wilkins SJ, Compton RG. Carbon nanotubes contain metal impurities which are responsible for the "electrocatalysis" seen at some nanotube-modified electrodes. Angew Chem Int Ed Engl. 2006;45(16):2533–7.
50. Jurkschat K, Ji X, Crossley A, Compton RG, Banks CE. Super-washing does not leave single walled carbon nanotubes iron-free. Analyst. 2007;132(1):21–3.
51. Hoffmann B, Seitz D, Mencke A, Kokott A, Ziegler G. Glutaraldehyde and oxidised dextran as crosslinker reagents for chitosan-based scaffolds for cartilage tissue engineering. J Mater Sci: Mater M. 2009;20(7):1495–503.
52. Hung TC, Giridhar R, Chiou SH, Wu WT. Binary immobilization of *Candida rugosa* lipase on chitosan. J Mol Catal B–Enzym. 2003;26:69–78.
53. Xu H, Dai H, Chen G. Direct electrochemistry and electrocatalysis of hemoglobin protein entrapped in graphene and chitosan composite film. Talanta. 2010;81:334–8.
54. Chávez-Servín JL, Castellote AI, López-Sabater MC. Analysis of mono- and disaccharides in milk-based formulae by high-performance liquid chromatography with refractive index detection. J Chromatogr A. 2004;1043:211–5.
55. Ning C, Segal S. Plasma galactose and galactitol concentration patients with galactose-1-phosphate uridyltransferase deficiency galactosemia: determination by gas chromatography/mass spectrometry. Metabolism. 2000;49:1460–6.
56. Çete S, Yaşar A, Arslan F. An amperometric biosensor for uric acid determination prepared from uricase immobilized in polypyrrole film. Artif Cell Nanomed Biotechnol. 2006;34:367–80.